

Journal of Materials Chemistry A

Accepted Manuscript



This is an *Accepted Manuscript*, which has been through the Royal Society of Chemistry peer review process and has been accepted for publication.

Accepted Manuscripts are published online shortly after acceptance, before technical editing, formatting and proof reading. Using this free service, authors can make their results available to the community, in citable form, before we publish the edited article. We will replace this *Accepted Manuscript* with the edited and formatted *Advance Article* as soon as it is available.

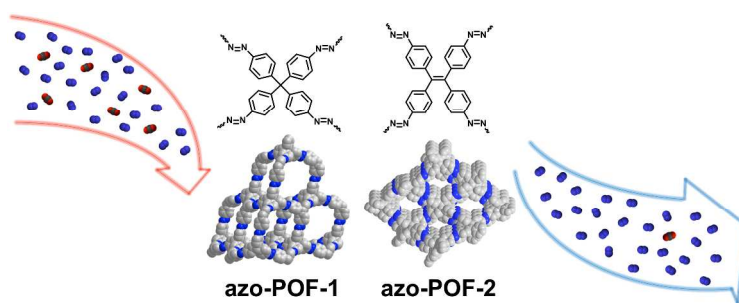
You can find more information about *Accepted Manuscripts* in the [Information for Authors](#).

Please note that technical editing may introduce minor changes to the text and/or graphics, which may alter content. The journal's standard [Terms & Conditions](#) and the [Ethical guidelines](#) still apply. In no event shall the Royal Society of Chemistry be held responsible for any errors or omissions in this *Accepted Manuscript* or any consequences arising from the use of any information it contains.

COMMUNICATION

Facile synthesis of azo-linked porous organic frameworks via reductive homocoupling for selective CO₂ capture

Graphical Abstract



Facile synthesis of azo-linked porous organic frameworks via reductive homocoupling for selective CO₂ capture

Cite this: DOI: 10.1039/x0xx00000x

Received 00th January 2012,
Accepted 00th January 2012Jingzhi Lu^a and Jian Zhang^{*a}

DOI: 10.1039/x0xx00000x

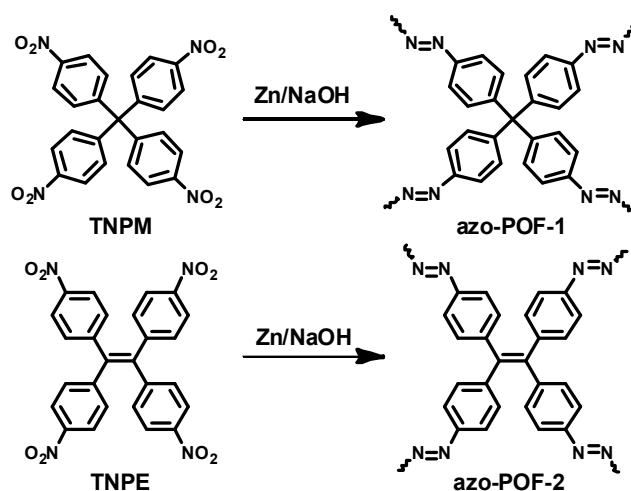
www.rsc.org/

A facile Zn-induced reductive homocoupling reaction was used to synthesize azo-linked porous organic frameworks (azo-POFs) from easily accessed nitro monomers. Azo-POF-2 exhibits the highest CO₂/N₂ selectivity of 76 at 273 K among all self-coupled azo-linked porous polymers.

Nanoporous organic polymers recently received increasing attention because of their high surface area, low density, wide structural tunability, and most of all, remarkable physicochemical stability resulting from the entirely covalently bonded networks.¹ They have emerged as a new class of highly desirable materials for practical applications in the storage and separation of a variety of gases including CO₂, which causes serious environmental concern due to its increasing atmospheric concentration.² For efficient postcombustion capture of CO₂, both adsorption capacity and CO₂/N₂ selectivity are important. Therefore, it is necessary to tailor the porosity parameters (surface area, pore volume, pore width, etc.) of porous polymers to achieve high adsorption capacity and/or selectivity. For example, increasing surface area and pore volume³ is often an effective method to improve adsorption capacity.⁴ Additionally, incorporating polar functional groups such as amine,⁵ aminal,⁶ imine,⁷ triazine,⁸ triazole,⁹ triethylene glycol monomethyl ether,¹⁰ and benzimidazole¹¹ can often enhance the CO₂/N₂ selectivity.¹² Azo-linked porous polymers based on -N=N- bonds are promising CO₂ adsorbents since their electron rich pore surfaces can lead to a high CO₂/N₂ selectivity.¹³ So far, azo-linked porous polymers have been synthesized either by heterocoupling between aromatic nitro and amine monomers^{13a, 13b} or by copper(I)-catalyzed oxidative homocoupling of aromatic amine monomers,^{13c} both of which require a reduction reaction of nitro compounds to prepare the amine monomers. Thus, a simple polymerization method which eliminates the use of amine monomers for synthesizing azo-linked porous polymers is highly desirable. In addition, the porous polymer accessed through the new method should ideally exhibit comparable CO₂/N₂ selectivity, if not higher, since it has been demonstrated that synthetic conditions can significantly affect the porosity parameters of porous polymers and correspondingly, their gas adsorption performance.¹⁴

Herein, we report the first example of synthesis of azo-linked porous organic frameworks (azo-POFs) using a facile Zn-induced

reductive homocoupling of aromatic nitro monomers. The obtained azo-POFs exhibit high CO₂/N₂ selectivity. In particular, azo-POF-2 shows the highest CO₂/N₂ selectivity of 76 (at 273 K) among all homocoupled, azo-linked porous polymers^{13c} despite its large pore width (1.5 nm). This suggests that an appropriate balance of surface area, pore width, and textural feature is required for a high CO₂/N₂ selectivity, which is of significant importance for the future rational design and synthesis of porous materials.



Scheme 1 Synthesis of azo-POFs via Zn-induced reductive coupling.

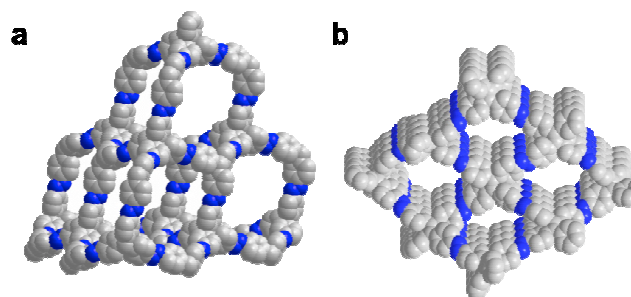


Fig. 1 Schematic illustration of (a) the *dia* topology of azo-POF-1 and (b) 4,4-connected 2D layers of azo-POF-2.

We adopted the classic zinc-induced reductive coupling of nitro compounds to synthesize azo-linked POFs since this method is mild, requires only one precursor, and can be performed under air.¹⁵ Two nitro compounds were chosen as the monomers based on their molecular geometry. Tetrakis(4-nitrophenyl)methane (TNPM) serves as a highly symmetric tetrahedral 4-connected building block. Ideally, a *dia* topology (Fig. 1a) is expected when it is polymerized via self-coupling reaction. 1,1,2,2-Tetrakis(4-nitrophenyl)ethane (TNPE), on the other hand, is also 4-connected but mostly planar, and we can expect an ideal, 4,4-connected, 2D layer is the targeted structure (Fig. 2a). The geometrical feature of the monomers induces a significant effect on the porosity parameters of the resulting porous polymers (*vide infra*). In a typical synthesis, the aromatic nitro monomer was dissolved in a solution containing THF, DMF, and NaOH, followed by adding freshly activated zinc powder (Scheme 1). The mixture was heated at 65 °C for 36 hours. The final product was washed by acid, water, acetone, and THF, followed by purification using Soxhlet extraction with water and THF. Common solvents used in the synthesis of azobenzene derivatives such as methanol and ethanol led to the formation of products with poor surface area (90 m²/g), probably due to the low solubility of monomers in such solvents. The ratio of THF and DMF was optimized to achieve the highest yield of azo-POFs. To confirm the importance of azo groups in CO₂ adsorption and CO₂/N₂ selectivity, we also prepared two other POFs (termed as ene-POFs) having the same scaffold structures as azo-POFs but contain -CH=CH- bonds, which lack the CO₂-philic moieties (see ESI for details of structure, synthesis, and characterization of ene-POFs).

Azo-POFs are insoluble in common organic solvents such as dichloromethane, acetone, THF, methanol, DMF, and DMSO, indicating they are cross-linked organic frameworks. Scanning electron microscopy (SEM) images (Fig. 2) show that both azo-POFs are mostly composed of particles of hundreds of nanometers. The amorphous nature of azo-POFs was also revealed by the broad diffraction peak in powder X-ray diffraction pattern (ESI, Fig. S9). The thermogravimetric analysis shows that the azo-POFs are stable in air below 350 °C and start losing mass above 350 °C due to the decomposition of the frameworks (Fig. S10). The presence of azo groups was revealed by Fourier transform infrared spectroscopy (FTIR) and cross-polarization magic-angle spinning (CP/MAS) ¹³C NMR. The FTIR spectra for azo-POFs show clear peaks at 1450 cm⁻¹ and 1405 cm⁻¹ (Fig. S1-S2), which can be assigned to the -N=N- stretching since the spectra of two model compounds show similar peaks at 1442 cm⁻¹ and 1402 cm⁻¹ (Fig. S1-S2, and see ESI for

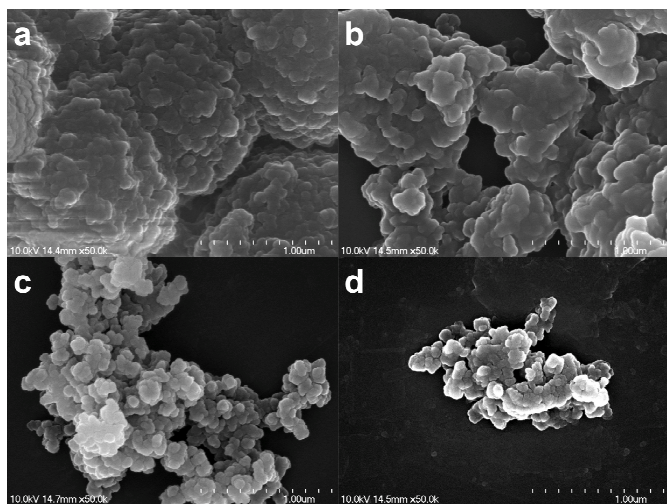


Fig. 2 SEM images of azo-POF-1 (a), azo-POF-2 (b), ene-POF-1 (c), and ene-POF-2 (d).

detailed synthesis and characterization of the model compounds). Furthermore, the chemical shifts in the CP/MAS ¹³C NMR spectra of azo-POF-1 and azo-POF-2 at 150.3 ppm and 151.4 ppm (Fig. S7-S8), respectively, are attributed to the carbon directly bonded to the azo group, consistent with previous reports.¹³ In addition, absorption bands at 1,520 and 1,340 cm⁻¹ in the FTIR spectra (Fig. S1-S2) indicate the presence of unreacted terminal nitro groups. This result is consistent with the elemental analysis, which shows a lower percentage of C, H, and N than expected (ESI).

The porosity of both azo-POFs and ene-POFs was investigated by nitrogen gas adsorption/desorption measurements at 77 K (Fig. 3). A rapid uptake at low pressure (0–0.1 bar) indicates a permanent microporous nature. The apparent hysteresis between adsorption and desorption suggests that all POFs are networks containing both meso- and micropores,¹⁶ which is attributed to the pore network effects, that is, mesopores are accessible only through micropores.¹⁷ Using Brunauer-Emmett-Teller (BET) model in the pressure range of $P/P_0 = 0.01–0.15$, the apparent surface areas (S_{BET}) were calculated as 712 m² g⁻¹ (azo-POF-1), 439 m² g⁻¹ (azo-POF-2), 755 m² g⁻¹ (ene-POF-1), and 622 m² g⁻¹ (ene-POF-2). It is also noted that POFs containing 3D linkage (tetrakisphenylmethane) exhibit higher surface areas than those containing 2D linkage (tetrakisphenylethene), a trend similar to a previous report of BILP polymers.^{11b} Pore-size distribution (Fig. 3b) based on nonlocal density functional theory (NLDFT) was estimated by fitting the N₂ adsorption isotherm, leading to pore sizes centered at 0.54, 1.50, 0.65, and 0.70 nm for azo-POF-1, azo-POF-2, ene-POF-1, and ene-POF-2, respectively. Indeed, the synthetic method significantly affects the porosity parameters of the resulting porous polymers. For example, azo-POF-1 has the same chemical structure as azo-COP-1 and ALP-2 that were previously synthesized using a metal-catalyst-free method^{13a, 13b} and a copper (I)-catalyzed method,^{13c} respectively, however, its S_{BET} is larger than that of azo-COP-1 (634 m² g⁻¹), but smaller than that of ALP-2 (1065 m² g⁻¹). In addition, the major pore width of azo-POF-1 (0.54 nm) is smaller than that of both azo-COP-1 (0.7 nm)^{13a, 13b} and ALP-2 (1.1 nm).^{13c}

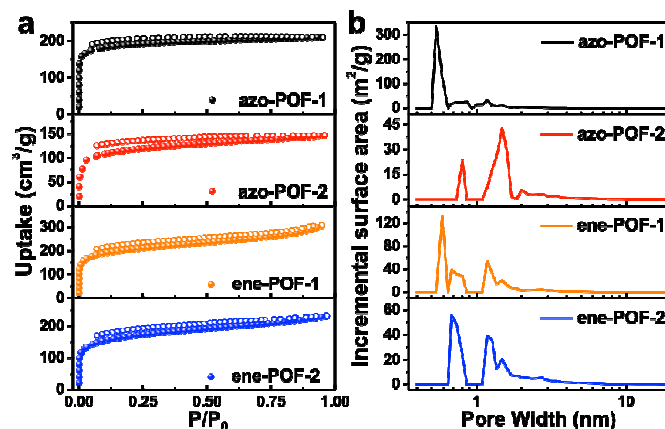


Fig. 3 N₂ uptake isotherm (a) and pore size distribution (b) of POFs at 77K. Filled and empty symbols represent adsorption and desorption, respectively.

We then collected CO₂ gas adsorption isotherms for both azo-POFs and ene-POFs at 273 K and 298 K (Table 1). Azo-POF-1 has the highest gravimetric CO₂ uptake of 131 mg g⁻¹ at 273 K and 1 bar, more than that of ene-POF-1 (86.4 mg g⁻¹) in spite of the latter's higher S_{BET} . The same result was also obtained when comparing the CO₂ uptake of azo-POF-2 (86.4 mg g⁻¹) and ene-FOF-2 (70.7 mg g⁻¹). Furthermore, a steeper rise at low pressure observed in the CO₂ isotherms of azo-POFs (Fig. 4) suggests a stronger binding energy of

azo groups, which was confirmed by the calculated isosteric heats of adsorption (Q_{st}).¹⁸ As shown in Table 1, the Q_{st} values at zero coverage are 27.5 and 26.2 kJ/mol for azo-POF-1 and azo-POF-2, respectively, higher than those of ene-POFs (24 kJ/mol), indicating the strong dipole-quadrupole interaction between the polarizable CO₂ molecules and the nitrogen sites on azo groups.¹⁹ Moreover, the moderate Q_{st} values of azo-POFs are weak enough to allow for material reactivation without applying heat, an attractive property since other materials with strong acidic or basic sites (e.g. alkanolamine) exhibiting high CO₂ affinities require large energy inputs to regenerate the active sites.²⁰

Table 1 CO₂ and N₂ uptakes, isosteric heats of adsorption, and CO₂/N₂ selectivity of POFs

polymer	CO ₂ ^a			N ₂ ^a		selectivity ^b	
	273 K	298 K	Q_{st}	273 K	298 K	273 K	298 K
azo-POF-1	131	82.9	27.5	5.4	4.4	69(52)	46(37)
azo-POF-2	84.5	55.1	26.6	3.2	2.6	76(55)	54(42)
ene-POF-1	86.4	50.0	24.5	3.6	2.9	50(43)	31(27)
ene-POF-2	70.7	40.2	24.6	2.8	2.1	54(48)	34(30)

^aGas uptake in mg g⁻¹ and the isosteric heats of adsorption (Q_{st}) in kJ mol⁻¹. ^bSelectivities (mg mg⁻¹) were calculated by initial slope method the selectivities (mg mg⁻¹, 1 bar) in parentheses were calculated IAST method as mole ratio of 15:85 for CO₂/N₂.

The CO₂/N₂ selectivities were calculated using both initial slope ratios estimated from Henry's law constants²¹ based on the pressure below 0.10 bar and the ideal adsorbed solution theory (IAST) based on single-component adsorption isotherms of CO₂ and N₂ collected at 273 and 298 K (Table 1 and ESI).²² At 273 K, ene-POFs exhibit lower selectivities (50-54) than azo-POFs, exemplifying again the importance of azo groups as polar functionalities to the high CO₂/N₂ selectivities of azo-linked polymers. The CO₂/N₂ selectivity of azo-POF-1 (69) is comparable to azo-COP-1 (73, 273 K)^{13a} and higher than ALP-2 (46, 273 K),^{13c} confirming that the facile Zn-induced reductive coupling method does not compromise the CO₂ adsorption of azo-POFs. Of particular interest is the high CO₂/N₂ selectivity of azo-POF-2 (76, 273 K). Generally, a small pore width is considered to be responsible for the high CO₂/N₂ selectivity, described as the

“sieving effect”.^{13c} Thus, it is quite unusual for azo-POF-2 (major pore width: 1.5 nm) exhibiting a high CO₂/N₂ selectivity of 76 when compared to azo-COP-1 (pore width: 0.7 nm, CO₂/N₂: 73)^{13a, 13b} and ALP-3 (pore width: 1.24 nm, CO₂/N₂: 68).^{13c} Hence, besides pore width, other pore metrics also contribute to the observed high CO₂/N₂ selectivity in azo-POF-2, which require further investigation. Recently, Yavuz *et al.* coined “N₂-phobicity” to describe the CO₂/N₂ selectivities of azo-COPs that increase as temperature increases.^{13a, 13b} This unusual phenomenon was attributed to the small pore width (0.4-0.8 nm) in azo-COPs, and pore width is the possible parameter that dictates the “N₂-phobicity”. It should be noted that although azo-POF-1 has the required narrow pore aperture, such “N₂-phobicity” was not observed. At 298 K, the CO₂/N₂ selectivity (estimated by initial slope method) of azo-POF-2 decreases to 54, which is still comparable to many other POFs with polar functional groups such as TPIs (31-56),²³ PECONFs (41-51),²⁴ and BILP-10 (59).²⁵ Importantly, CO₂/N₂ selectivities predicted by IAST method at both 273 K and 298 K (Table 1) show consistent trend among four POFs: azo-POF-2 exhibit the highest selectivity of 55 (273 K) and 42 (298 K). These values are lower than those of azo-COPs (96-131),^{13a} but higher than several well studied porous polymers including CTFs (14-31),²⁶ PCTFs (14-41),²⁷ PPFs (15-20),⁷ MOPs (8-25),²⁸ etc.

In conclusion, we successfully synthesized two azo-linked porous organic frameworks (azo-POFs) using a facile Zn-induced reductive homocoupling of aromatic nitro monomers. Azo-POFs have a moderate BET surface area (up to 712 m² g⁻¹) but good CO₂ uptake (up to 13.1 wt% at 273 K and 1 bar) due to the electron-rich pore surface. Surprisingly, azo-POF-2, prepared in our work, exhibits the highest CO₂/N₂ selectivity (76 at 273 K) in spite of its largest average pore width among all self-coupled azo-linked frameworks (azo-POFs and ALPs). It suggests that pore width should be considered in combination with other porosity parameters such as surface area, pore polarity, and textural features resulting from a specific synthetic method to account for the ultimate CO₂/N₂ selectivity of a particular POF. Continuous investigation on the effect of internal pores' chemical environment on the CO₂/N₂ selectivity of azo-POFs is currently underway in our lab.

We acknowledge financial support from the University of Nebraska-Lincoln and Nebraska Center for Energy Sciences Research. J. Z. is also grateful for the Donors of the American Chemical Society Petroleum Research Fund for partial support of this research. We thank Dr. Dewey Barich for the assistance in CP/MAS ¹³C NMR measurements.

Notes and references

^a Department of Chemistry, University of Nebraska-Lincoln, Lincoln, NE 68588, USA. E-mail: jzhang3@unl.edu

† Electronic Supplementary Information (ESI) available: Experimental procedures, characterization methods, and gas adsorption studies. See DOI: 10.1039/c000000x/

- (a) D. Wu, F. Xu, B. Sun, R. Fu, H. He and K. Matyjaszewski, *Chem. Rev.*, 2012, **112**, 3959; (b) R. Dawson, A. I. Cooper and D. J. Adams, *Prog. Polym. Sci.*, 2012, **37**, 530; (c) Y. Xu, S. Jin, H. Xu, A. Nagai and D. Jiang, *Chem. Soc. Rev.*, 2013, **42**, 8012; (d) X. Zou, H. Ren and G. Zhu, *Chem. Commun.*, 2013, **49**, 3925; (e) Y. Jin, Y. Zhu and W. Zhang, *CrystEngComm*, 2013, **15**, 1484.
- R. Monastersky, *Nature*, 2013, **497**, 13.
- (a) B. G. Hauser, O. K. Farha, J. Exley and J. T. Hupp, *Chem. Mater.*, 2013, **25**, 12; (b) R. K. Totten, Y. S. Kim, M. H. Weston, O. K. Farha, J. T. Hupp and S. T. Nguyen, *J. Am. Chem. Soc.*, 2013, **135**, 11720; (c) A. Gorrirane, A. Corma and H. Garcia, *Nat. Protoc.*, 2010, **5**, 429.
- D. Yuan, W. Lu, D. Zhao and H. C. Zhou, *Adv. Mater.*, 2011, **23**, 3723.

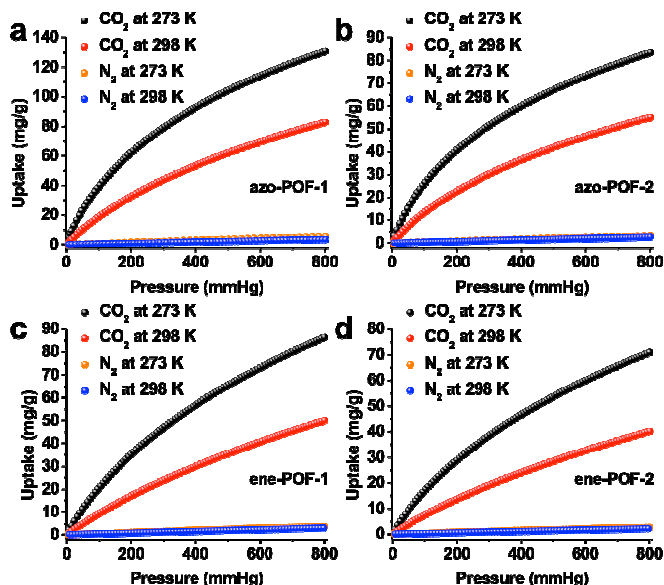


Fig. 4 CO₂ and N₂ uptake isotherms of azo-POFs and ene-POFs at 273 K and 298 K.

5. (a) E. Merino, E. Verde-Sesto, E. M. Maya, M. Iglesias, F. Sánchez and A. Corma, *Chem. Mater.*, 2013, **25**, 981; (b) W. Lu, D. Yuan, J. Sculley, D. Zhao, R. Krishna and H. C. Zhou, *J. Am. Chem. Soc.*, 2011, **133**, 18126; (c) W. Lu, J. P. Sculley, D. Yuan, R. Krishna, Z. Wei and H. C. Zhou, *Angew. Chem., Int. Ed.*, 2012, **51**, 7480.
6. M. G. Schwab, B. Fassbender, H. W. Spiess, A. Thomas, X. Feng and K. Mullen, *J. Am. Chem. Soc.*, 2009, **131**, 7216.
7. Y. Zhu, H. Long and W. Zhang, *Chem. Mater.*, 2013, **25**, 1630.
8. J. Roeser, K. Kailasam and A. Thomas, *ChemSusChem*, 2012, **5**, 1793.
9. P. Pandey, O. K. Farha, A. M. Spokoyny, C. A. Mirkin, M. G. Kanatzidis, J. T. Hupp and S. T. Nguyen, *J. Mater. Chem.*, 2011, **21**, 1700.
10. Y. Jin, B. A. Voss, R. McCaffrey, C. T. Baggett, R. D. Noble and W. Zhang, *Chem. Sci.*, 2012, **3**, 874.
11. (a) M. G. Rabbani and H. M. El-Kaderi, *Chem. Mater.*, 2011, **23**, 1650; (b) M. G. Rabbani and H. M. El-Kaderi, *Chem. Mater.*, 2012, **24**, 1511; (c) M. G. Rabbani, T. E. Reich, R. M. Kassab, K. T. Jackson and H. M. El-Kaderi, *Chem. Commun.*, 2012, **48**, 1141.
12. R. Dawson, A. I. Cooper and D. J. Adams, *Polym. Int.*, 2013, **62**, 345.
13. (a) H. A. Patel, S. H. Je, J. Park, D. P. Chen, Y. Jung, C. T. Yavuz and A. Coskun, *Nat. Commun.*, 2013, **4**, 1357; (b) H. A. Patel, S. H. Je, J. Park, Y. Jung, A. Coskun and C. T. Yavuz, *Chem.-Eur. J.*, 2014, **20**, 772; (c) P. Arab, M. G. Rabbani, A. K. Sekizkardes, T. İslamoğlu and H. M. El-Kaderi, *Chem. Mater.*, 2014, **26**, 1385.
14. A. Bhunia, V. Vasylyeva and C. Janiak, *Chem. Commun.*, 2013, **49**, 3961.
15. H. E. Bigelow and D. B. Robinson, *Org. Synth.*, 1942, 28.
16. J. Jeromenok and J. Weber, *Langmuir*, 2013, **29**, 12982.
17. P. M. Budd, E. S. Elabas, B. S. Ghanem, S. Makhseed, N. B. McKeown, K. J. Msayib, C. E. Tattershall and D. Wang, *Adv. Mater.*, 2004, **16**, 456.
18. J. L. Rowsell and O. M. Yaghi, *J. Am. Chem. Soc.*, 2006, **128**, 1304.
19. D. M. D'Alessandro, B. Smit and J. R. Long, *Angew. Chem., Int. Ed.*, 2010, **49**, 6058.
20. G. T. Rochelle, *Science*, 2009, **325**, 1652.
21. (a) R. Banerjee, H. Furukawa, D. Britt, C. Knobler, M. O'Keeffe and O. M. Yaghi, *J. Am. Chem. Soc.*, 2009, **131**, 3875; (b) J. An, S. J. Geib and N. L. Rosi, *J. Am. Chem. Soc.*, 2010, **132**, 38.
22. A. L. Myers and J. M. Prausnitz, *AIChE J.*, 1965, **11**, 121.
23. M. R. Liebl and J. Senker, *Chem. Mater.*, 2013, **25**, 970.
24. P. Mohanty, L. D. Kull and K. Landskron, *Nat. Commun.*, 2011, **2**, 401.
25. M. G. Rabbani, A. K. Sekizkardes, O. M. El-Kadri, B. R. Kaafarani and H. M. El-Kaderi, *J. Mater. Chem.*, 2012, **22**, 25409.
26. S. Ren, M. J. Bojdys, R. Dawson, A. Laybourn, Y. Z. Khimyak, D. J. Adams and A. I. Cooper, *Adv. Mater.*, 2012, **24**, 2357.
27. A. Bhunia, I. Boldog, A. Möller and C. Janiak, *J. Mater. Chem. A*, 2013, **1**, 14990.
28. R. Dawson, E. Stöckel, J. R. Holst, D. J. Adams and A. I. Cooper, *Energy Environ. Sci.*, 2011, **4**, 4239.

Journal Name

RSCPublishing

COMMUNICATION

Journal of Materials Chemistry A Accepted Manuscript